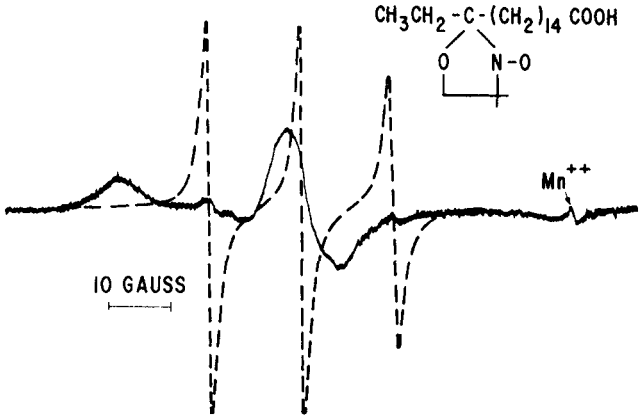


**Fig. 3. The ESR spectrum of 2-(14-carboxytetradecyl)-2-ethyl-4, 4-dimethyl-3-oxazolidinyloxyl (spin labeled fatty acid). Dashed spectrum is of 100 p.p.m. spin label dissolved in silicone fluid SF-96 (100). Solid spectrum is of 100 p.p.m. spin label dissolved in silicone fluid SF-96 (100) containing 5% dispersed Santocel C silica. The two spectra indicate that the spin label is strongly adsorbed by the Santocel C. Both samples were purged with nitrogen for 10 min at 60°C to reduce dissolved oxygen. The g value for the $Mn^{++}$ marker is 1.981. The unpaired electron on the spin labeled fatty acid is localized near the N atom.**

The effect of dispersing 5% Santocel C silica, as shown in Figure 2, was to lower $\Pi_s$ by about 2 dynes/cm. According to Ross (1967), this lower $\Pi_s$ would not be expected to increase antifoam effectiveness. All other things being equal, a lower spreading pressure would be expected to decrease antifoam effectiveness. The lowering of $\Pi_s$ by Santocel C was observed regardless of the dispersion preparation method.

Figure 2 also presents the II-A data for SF-96 (100) equilibrated with coarse (6 to 16 mesh) silica gel. The marked lowering of $\Pi_s$ by the silica gel suggested that Santocel C silica also lowers $\Pi_s$ via the adsorption of surface active impurities. In all three cases, presented in Figure 2, the SF-96 (100) was from the same 1 gal. sample, eliminating any uncertainties about the relative level of impurities.

The conclusion that Santocel C reduces $\Pi_s$ by adsorption of surface active impurities was further supported by the electron spin resonance spectra of a spin labeled fatty acid in SF-96 (100) and in a dispersion of 5% Santocel C in SF-96 (100). These spectra, presented in Figure 3, clearly show that the spin labeled fatty acid is strongly immobilized by the Santocel C. For a more detailed explanation of the spin label method, McConnell and McFarland (1970), and Smith (1970) should be consulted.

The SF-96 (100) equilibrated with coarse mesh silica gel did not show any improved antifoam effectiveness. Therefore, the adsorption or removal of surface active impurities cannot account for the effect of Santocel C in improving antifoam effectiveness.

From Figure 1 it is seen that the viscosity of SF-96 (100) increases with the amount of dispersed silica. Thus, it may be suggested that the increase in viscosity is responsible for the subsequent increase in antifoam effectiveness. However, an antifoam prepared from silica free 350 centistokes silicone fluid was no more effective than antifoam prepared from silica free 100 centistokes silicone fluid.

In summary, the addition of Santocel C silica to silicone fluid SF-96 (100) lowers the spreading pressure about 2 dynes/cm. This lowering is most likely due to the adsorption of surface active impurities, as demonstrated by the effect of coarse mesh silica gel and by electron spin resonance. Santocel C also increases the viscosity of silicone fluids. However, neither the lower spreading pressure, the adsorption of impurities, nor the increase in viscosity can be related to the increase in antifoam effectiveness.

## NOTATION

$A$ = area of monolayer film
$L$ = position of barrier on Cenco film balance
$L_o$ = initial position of barrier on Cenco film balance
$\Pi$ = monolayer film pressure
$\Pi_s$ = spreading pressure

## ACKNOWLEDGMENT

Appreciation is expressed to G. L. Gaines, Jr., for helpful advice and discussions and to W. Raleigh and R. Ronda of General Electric Silicone Products Department for graciously providing antifoam ingredients, samples and specially prepared antifoam compounds and for performing the defoam tests and viscosity measurements presented in Figure 1.

## LITERATURE CITED

Bikerman, J. J., *Foams*, Springer-Verlag, New York (1973).
Corrin, M. L., "The Specific Surface Area and Nitrogen Interaction Energy of Various Solids," *General Electric Company Research Report RL-801* (1953).
McConnell, H. M., and B. G. McFarland, "Physics and Chemistry of Spin Labels," *Quart. Rev. Biophysics*, 3, 91 (1970).
Pomerantz, P., et al., "Spreading Pressures and Coefficients, Interfacial Tensions, and Adhesion Energies of the Lower Alkanes, Alkenes, and Alkyl Benzenes on Water," *J. Colloid Interface Sci.*, 24, 16 (1967).
Ross, S., "Mechanisms of Foam Stabilization and Antifoaming Action," *Chem. Eng. Progr.*, 63, 41 (1967).
Smith, Ian C. P., "The Spin Lable Method," in *Biological Applications of ESR Spectroscopy*, John Wiley-Interscience, New York (1970).

*Manuscript received February 12, 1975; revision received May 15, and accepted May 16, 1975.*

# The Stability of Nuclei Generated by Contact Nucleation

**R. W. ROUSSEAU, W. L. McCABE and C. Y. TAI**

**Department of Chemical Engineering**
**North Carolina State University**
**Raleigh, North Carolina 27607**

Tai et al. (1975) studied contact nucleation of $MgSO_4 \cdot 7H_2O$, $KAl(SO_2)_2 \cdot 12H_2O$, $K_2SO_4$, and citric acid. In their experiments, the crystal was impacted with a stainless steel rod; the resulting nuclei were swept away from the crystal face by the flowing solution and allowed to develop in a growth chamber. The supersaturation in the chamber was held at the same level as that at which the crystal impact occurred. Their results clearly showed

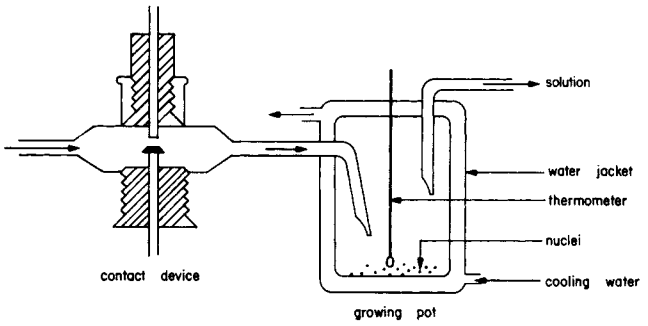


Fig. 1. Contacting and growth chambers.

that the number of nuclei generated by single impact was a function of the supersaturation in the system. The form of the function used to correlate the number of nuclei and supersaturation was the same as that used to relate crystal growth rate and supersaturation. Since both growth rate and contact nucleation may be considered surface phenomena, the relationship implied by this observation was not completely surprising.

Garbedian and Strickland-Constable (1972) reported a series of experiments in which a single cured sodium chlorate seed crystal was caused to slide across a glass surface in an aqueous solution at a fixed supersaturation. After the sliding had ceased, the solution was diluted to varying degrees of supersaturation and the resulting nuclei allowed to grow to visible size. The results of these experiments indicate that the number of nuclei which survive to a visible size is dependent on the supersaturation of the solution during the development period.

Randolph and Sikdar (1974) reviewed numerous systems which exhibit large numbers of very small crystals which exist in the magma of stirred tank crystallizers but do not survive to populate larger size fractions. These authors considered four reasons for their observations:

1. Population measurements at small sizes were in error.
2. Nuclei became attached to parent crystals.
3. Secondary nuclei were unstable such that the majority dissolved.
4. There was low growth rate at the small sizes which resulted in high crystal washout.

Randolph and Sikdar (1974) present data for potassium sulfate which led them to conclude that the first three of the possibilities were not important, and the significance of the fourth was questionable.

## EXPERIMENTAL

To test the stability of the nuclei generated by a crystal-solid impact, the apparatus shown in Figure 1 was constructed. The growing pot had a total volume of approximately 300 ml. Tai et al. (1975) give a schematic of the entire apparatus and present a discussion of the crystal counting procedure. A series of experiments was conducted in which the saturation and crystal temperatures were held constant, while the temperature $T_G$ at which the nuclei grew to visible size was varied. The impact energy was constant for all experiments. The system studied was an aqueous solution of $KAl(SO_4) \cdot 12H_2O$.

## RESULTS AND DISCUSSION

Despite the fact that it took the solution temperature 4 to 5 min. to stabilize after it had entered the growth chamber, the number of nuclei which grew to a visible size varied markedly with $T_G$. These results are shown in Figures 2 and 3. The variation between the two curves is believed due to a slight misalignment in the contacting

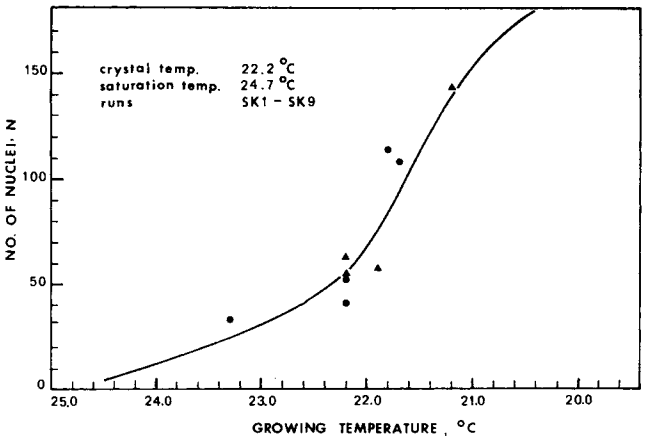


Fig. 2. Effect of development temperature on the $KAl(SO_4)_2 \cdot 12\ H_2O$ nuclei which survive.

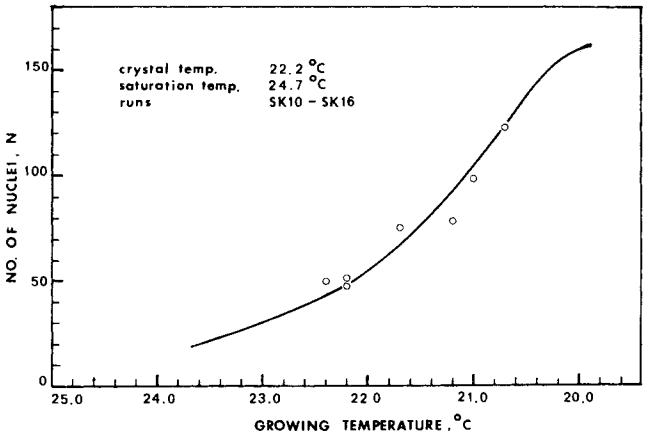


Fig. 3. Effect of development temperature on the $KAl(SO_4)_2 \cdot 12\ H_2O$ nuclei which survive (new crystal).

device and the crystal face; this should have no bearing on the objectives of the experiments.

These data follow the observations of Garabedian and Strickland-Constable (1972) and lend support to what has been termed the survival theory. This theory is based on the Gibbs-Thomson equation which at low supersaturations reduces to

$$\alpha - 1 = \frac{2\sigma V}{RT}\,\frac{1}{r_o} \tag{1}$$

where $r_o$ is the size of a critical nucleus; that is, crystals of a size smaller than $r_o$ dissolve while those greater than $r_o$ survive.

As suggested by Ottens (1973), the particles generated by an impact are distributed over a size range; Randolph and Cise (1972) suggest that these particle sizes may be described by a gamma distribution function

$$B(L) = B^o\,\frac{L^a \exp\left(-\dfrac{aL}{b}\right)}{\Gamma(1+a)\left(\dfrac{b}{a}\right)^{a+1}} \tag{2}$$

If the system supersaturation is set so that the size of a critical nucleus is $r_o$, then the fraction of particles which survive, $f_s$, is given by

$$f_s = \frac{B_s^o}{B^o} = \int_{r_o}^{\infty} \frac{L^a \exp\left(-\dfrac{aL}{b}\right)}{\Gamma(1+a)\left(\dfrac{b}{a}\right)^{a+1}}\,dL \tag{3}$$

This integral is an incomplete gamma function $Q(a, r_o)$. In this function $a$ is a measure of the spread of the distribution which presumably would not vary for the experiments described earlier. As already pointed out, however, $r_o$ will vary with the temperature of the growth chamber, and it seems plausible that the curves shown in Figures 2 and 3 are portions of a cumulative distribution function such as that given by Equation (3).

The evidence points towards a dual role for the influence of supersaturation on contact nucleation. First, the system supersaturation influences the growth rate which in turn may be reflected in the nature of the crystal face. If the face becomes rougher or softer with a change in supersaturation, a given impact will produce more particles resulting in a higher observed rate of nucleation. Second, the system supersaturation influences the fraction of the particles produced by an impact which survive. It becomes more important to distinguish between these two factors for a crystallization process where supersaturation may not be uniform throughout the equipment, as would be the case for fines dissolution or clear liquor advance.


#### ACKNOWLEDGMENT

The support of the National Science Foundation under Grant GK-39002 is gratefully acknowledged.


#### NOTATION

$a, b$ = constants in the distribution function of particles generated by a crystal impact
$B^o$ = total number of particles generated by an impact
$B_s^o$ = number of particles which survive to macroscopic size
$B(L)$ = the distribution function of particles generated by a crystal impact
$f_S$ = fraction of particles which survive
$L$ = characteristic length of crystals
$Q(a, r_o)$ = incomplete gamma function
$r_o$ = critical length of a nucleus
$R$ = gas constant
$T$ = system temperature
$V$ = molar volume of the crystalline substance
$y_A$ = mole fraction of solute in liquid
$y_{A,S}$ = saturation mole fraction of solute at the system temperature
$\alpha$ = supersaturation ratio, $y_A/y_{A,S}$
$\Gamma(1 + a)$ = gamma function
$\sigma$ = interfacial energy

#### LITERATURE CITED


Garabedian, H., and R. F. Strickland-Constable, "Collision Breeding of Crystal Nuclei: Sodium Chlorate. I," *J. Crystal Growth*, **12**, 53 (1972).

Ottens, E. P. K., Ph.D. dissertation, Technological University of Delft, Delft, The Netherlands (1973).

Randolph, A. D., and M. D. Cise, "Nucleation Kinetics of the Potassium Sulfate-Water Systems," *AIChE J.*, **18**, 798 (1972).

Randolph, A. D., and S. K. Sikdar, "Survival of Secondary Crystall Nuclei of $K_2SO_4$," GVC/AIChE-Joint Meeting, Munich, Preprints Vol. 1, A5-3(1974).

Tai, C. Y., W. L. McCabe, and R. W. Rousseau, "Contact Nucleation of Various Crystal Types," *AIChE J.*, **21**, 351 (1975).



*Manuscript received June 6, 1975; revision received July 3, and accepted July 8, 1975.*


# Oscillations on Sieve Trays


**W. VAL PINCZEWSKI and CHRISTOPHER J. D. FELL**

**School of Chemical Engineering, University of New South Wales N.S.W. 2033, Australia**


In several recent articles Biddulph and Stephens (1974) and Biddulph (1975) have studied lateral oscillations occurring on distillation sieve trays. They have identified two types of stable oscillation which they term "full wave" and "half wave," respectively. In full-wave oscillations, the dispersion on both sides of the tray simultaneously moves towards the tray center and then back again. In half-wave oscillations, the liquid on the tray sloshes from side to side. At gas loadings intermediate between those to initiate either type of oscillation, the nature of the biphase on the tray becomes confused with peaks moving around the tray. From a tray design viewpoint, the presence of half-wave oscillations in particular is shown to be undesirable, as tray entrainment may be increased by as much as 70%.

Biddulph and Stephens (1974) have found that the experimental initiation points for both types of oscillation can be satisfactorily correlated by the group

$$B_S = \frac{V\epsilon h_f \rho_g}{g d^3 \rho_L \bar{\alpha}} \qquad (1)$$

with $B_S$ taking the value $0.5 \times 10^{-5}$ for full-wave oscillations and $2.5 \times 10^{-5}$ for half-wave oscillations. The cube root of the ratio of the critical values of $B_S$ is 1.71 compared with the expected value of 2.0 based on the hypothesis that half-wave oscillations occur at double the wavelength for full-wave oscillations. No satisfactory explanation is offered for this apparent discrepancy.

However, a closer examination of available experimental evidence on the gas velocity at the initiation point for half-wave oscillations reveals that this velocity closely corresponds to the velocity at which phase inversion occurs on the tray. This can be seen from Table 1 in which reported gas velocities at the half-wave initiation point (expressed in terms of $F_S$, the tray superficial $F$ factor based on active area) are compared with predicted superficial $F$ factors for the phase inversion point.

This, therefore, suggests that the appearance of half-wave oscillations is coincident with phase inversion on the tray and that the initiation velocity for half-wave oscillations corresponds to the velocity at which the dispersion on the tray is primarily a spray (that is, to the velocity at phase inversion or the froth to spray transition). The apparent discrepancy in the critical $B_S$ values of Biddulph and Stephens (1974) may be simply explained. Since with phase inversion the nature of the dispersion changes from liquid continuous to gas contin-


Correspondence concerning this paper should be addressed to Christopher J. D. Fell, Department of Chemical Engineering, University of Illinois, Urbana, Illinois 61801. W. Val Pinczewski is with Esso Australia, Ltd., Sydney, Australia.